Environmental Science & Technology

Article

Cite This: Environ. Sci. Technol. 2019, 53, 8695−8705

pubs.acs.org/est

Specific Micropollutant Biotransformation Pattern by the Comammox Bacterium *Nitrospira inopinata*

Ping Han,[†,‡,§,$] Yaochun Yu,[∥,$] Lijun Zhou,[§,⊥] Zhenyu Tian,[#] Zhong Li,[¶] Lijun Hou,[†] Min Liu,[‡] Qinglong Wu,[⊥,□] Michael Wagner,[§,■,▽] and Yujie Men*[,∥,◆]

[†]State Key Laboratory of Estuarine and Coastal Research, [‡]Key Laboratory of Geographic Information Science (Ministry of Education), East China Normal University, 500 Dongchuan Road, Shanghai 200241, China

[§]Centre for Microbiology and Environmental Systems Science, Division of Microbial Ecology, University of Vienna, Althanstrasse 14, 1090 Vienna, Austria

[∥]Department of Civil and Environmental Engineering, University of Illinois at Urbana-Champaign, Urbana, Illinois 61801, United States

[⊥]State Key Laboratory of Lake Science and Environment, Nanjing Institute of Geography and Limnology, Chinese Academy of Sciences, Nanjing 210008, China

[#]Center for Urban Waters, University of Washington Tacoma, Tacoma, Washington 98421, United States

[¶]Metabolomics Center, University of Illinois, Urbana, Illinois 61801, United States

[□]Sino-Danish Center for Education and Science, University of Chinese Academy of Science, Beijing 100190, China

[■]The Comammox Research Platform of the University of Vienna, 1090 Vienna, Austria

[▽]Department of Biotechnology, Chemistry and Bioscience, Aalborg University, 9100 Aalborg, Denmark

[◆]Institute for Genomic Biology, University of Illinois at Urbana-Champaign, Urbana, Illinois 61801, United States

Supporting Information

ABSTRACT: The recently discovered complete ammonia-oxidizing (comammox) bacteria occur in various environments, including wastewater treatment plants. To better understand their role in micropollutant biotransformation in comparison with ammonia-oxidizing bacteria (AOB) and ammonia-oxidizing archaea (AOA), we investigated the biotransformation capability of *Nitrospira inopinata* (the only comammox isolate) for 17 micropollutants. Asulam, fenhexamid, mianserin, and ranitidine were biotransformed by *N. inopinata*, *Nitrososphaera gargensis* (AOA), and *Nitrosomonas nitrosa* Nm90 (AOB). More distinctively, carbendazim, a benzimidazole fungicide, was exclusively biotransformed by *N. inopinata*. The biotransformation of carbendazim only occurred when *N. inopinata* was supplied with ammonia but not nitrite as the energy source. The exclusive biotransformation of carbendazim by *N. inopinata* was likely enabled by an enhanced substrate promiscuity of its unique AMO and its much higher substrate (for ammonia) affinity compared with the other two ammonia oxidizers. One major plausible transformation product (TP) of carbendazim is a hydroxylated form at the aromatic ring, which is consistent with the function of AMO. These findings provide fundamental knowledge on the micropollutant degradation potential of a comammox bacterium to better understand the fate of micropollutants in nitrifying environments.

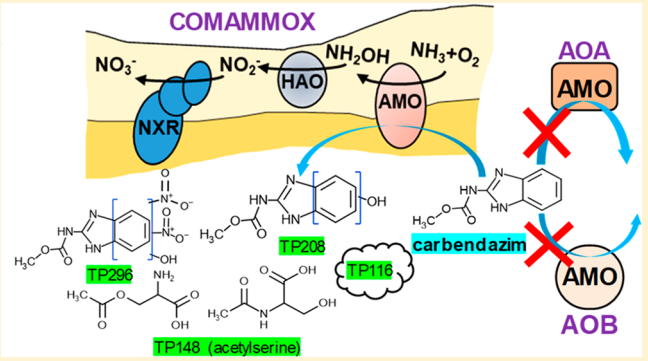

INTRODUCTION

Micropollutants including pesticides, pharmaceuticals, and personal care products, which occur at low levels (ng−μg/L) are a considerable environmental concern due to their potential adverse effects on ecosystems and human health.[1−4] Therefore, it is important to obtain an in-depth understanding of the environmental fate of these compounds. Biotransformation of micropollutants plays an essential role in their removal, particularly in wastewater treatment plants (WWTPs), and has recently been extensively investigated.[3,5,6] More specifically, biotransformation of various micropollutants is associated with ammonia oxidation activity of nitrifying activated sludge and biofilms in WWTPs.[5,7−14] Consistently, biotransformation of

Received: February 18, 2019
Revised: June 29, 2019
Accepted: July 11, 2019
Published: July 11, 2019

DOI: 10.1021/acs.est.9b01037
Environ. Sci. Technol. 2019, 53, 8695−8705

some micropollutants is catalyzed by enriched or pure cultures of ammonia-oxidizing microbes.[15,16]

Ammonia-oxidizing bacteria (AOB) are typically the dominant ammonia oxidizers in municipal WWTPs.[17−19] Ammonia-oxidation is initiated by ammonia monooxygenases (AMO), a substrate promiscuous key enzyme[20−23] of all known ammonia oxidizers. Some AOB metabolically or cometabolically catalyze the transformation of various compounds including polycyclic aromatic hydrocarbons and pharmaceuticals.[6,12,20,22,24,25] Besides AOB, ammonia-oxidizing archaea (AOA) have also been molecularly detected and/or cultured in nitrifying activated sludge of some industrial and municipal WWTPs.[19,26−29] In 2015, complete ammonia oxidizers (comammox), which as single organisms oxidize ammonia all the way to nitrate via nitrite, were discovered.[30,31] Phylogenetic analyses revealed that the *amoA* genes of comammox bacteria differ from those of known AOB and AOA species and represent a distinct lineage of AMO enzymes within this enzyme family.[30] All known comammox bacteria belong to the genus *Nitrospira* and have been detected in various environments including WWTPs.[30−34] *Nitrospira inopinata* is the only comammox isolate available to date and has a much higher affinity for ammonia than many AOA and all tested AOB.[35] The distinct enzymatic repertoire of comammox bacteria, as well as their high substrate affinity, might enable them to perform important ecological services in natural and engineered environments, which have not yet been well understood.

A series of recent studies provided additional insights into the mechanisms behind micropollutant degradation by AOB and AOA.[16,36] Two AOB strains, *Nitrosomonas nitrosa* Nm90 and *Nitrosomonas* sp. Nm95 isolated from industrial sewage,[37] and the AOA strain, *Nitrososphaera gargensis* isolated from a hot spring effluent mat,[38,39] showed biotransformation of two pharmaceuticals (mianserin and ranitidine) through cometabolism likely mediated by AMO upon ammonia oxidation.[16] Consistently, biotransformation of 31 out of 79 structurally different micropollutants was inhibited after application of AMO inhibitors in a nitrifying activated sludge community.[8] A follow-up study revealed that a portion of micropollutants whose biotransformation was associated with nitrification was biotransformed by the AOB *Nitrosomonas europaea* via both cometabolic biotransformation by AMO and abiotic transformation by hydroxylamine, an intermediate produced by AMO during ammonia oxidation.[40]

Nothing is yet known about the role of comammox bacteria in the turnover of micropollutants. Differences in biotransformation activities of these microbes compared to AOB and AOA might be expected, as they possess unique AMO enzymes and the complete enzyme set for nitrification. As comammox bacteria are widespread in WWTPs, targeted studies exploring their potential contribution to micropollutant biotransformation associated with nitrification are needed to better understand the fate of those micropollutants during wastewater treatment and in other nitrifying environments. The goal of this study was to expand the fundamental knowledge on micropollutant biotransformation potential of different ammonia oxidizers in isolation, with a focus on the newly discovered comammox bacteria. We selected 17 commonly used pharmaceuticals and pesticides whose biotransformation was inhibited by more than 20% when adding AMO inhibitors in a nitrifying activated sludge community.[8] The biotransformation of these micropollutants by the comammox isolate *N. inopinata* was tested and compared with the biotransformation by the AOA *N. gargensis* and the AOB *N. nitrosa* Nm90. Two pharmaceuticals (mianserin and ranitidine) that are biotransformed by *N. gargensis* and *N. nitrosa* Nm 90[16] were also included to study their degradability by *N. inopinata*. Transformation products (TPs) were identified, and the mechanisms of MPs biotransformation by *N. inopinata* and the responsible enzyme(s) were further investigated.

MATERIALS AND METHODS

Micropollutant Selection. The target micropollutants (i.e., acetamiprid, asulam, bezafibrate, carbendazim, clomazone, fenhexamid, furosemide, indomethacin, irgarol, levetiracetam, mianserin, monuron, ranitidine, rufinamide, tebufenozide, thiacloprid, and trimethoprim) were selected based on the following criteria: (1) their biotransformation was inhibited >20% by AMO inhibitors in a previous activated sludge study;[8] (2) the reference standards are commercially available. A complete list of the investigated micropollutants and their applications can be found in Table S1. The reference standards of selected micropollutants were purchased from Sigma-Aldrich (St. Louis, MO) and Toronto Research Chemicals (Toronto, Canada). Five internal standards: trimethoprim-d_3, metoprolol acid-d_5, carbendazim-d_4, and furosemide-d_5 were obtained from C/D/N Isotopes (Quebec, Canada) and Toronto Research Chemicals (Toronto, Canada). Stock solutions of all tested compounds were prepared in methanol with a concentration of 1 g/L, except for carbendazim (0.25 g/L), and stored at −20 °C until use. Given the potential inhibitory effects of these micropollutants on ammonia oxidizers,[16,40] we divided the 17 micropollutants into two groups (i.e., group A and group B) to reduce the total number of micropollutants and the total concentration in the mixtures. Micropollutants in each group were added as a mixture.

Cultivation of Microorganisms. All strains were maintained in the same modified basal medium[35] with 4 g/L $CaCO_3$ for buffering the pH at ∼8.0. *N. inopinata* was incubated at 42 °C in the dark without shaking, and 2 mM NH_4Cl was added as growth substrate periodically upon depletion (∼every 7 days). *N. gargensis* was incubated at 46 °C in the dark without shaking, and 2 mM NH_4Cl was added as growth substrate ∼every 6 days. *N. nitrosa* Nm90 was obtained from the AOB strain collection of the University of Hamburg (Germany)[37] and was incubated at 37 °C in the dark with shaking at 90 rpm, amended with 2 mM NH_4Cl every ∼6 days. The nitrite-oxidizing bacterium *Nitrospira defluvii*[41] was incubated at 37 °C in the dark without shaking, and 1 mM $NaNO_2$ was added as growth substrate every ∼7 days.

Micropollutant Biotransformation Screening. The micropollutant biotransformation capabilities of the comammox *N. inopinata*, AOA *N. gargensis*, and AOB *N. nitrosa* Nm90 were investigated in batch experiments. Pregrown biomass was harvested by centrifugation at 7380 × *g* for 30 min at 10 °C, and the pellet was resuspended in fresh medium to obtain 2-fold concentrated biomass. In our previous study, the concentration of MPs in WWTPs ranges from several ng/L to less than a hundred μg/L.[14] Thus, the corresponding volume of mixed micropollutant stock solutions to reach an initial concentration of 20 μg/L (for each micropollutant) was first added into empty sterile bottles. After the organic solvent methanol was evaporated, 25 mL of thoroughly mixed concentrated culture with 2 mM NH_4Cl was inoculated into 100 mL glass bottles, respectively. NH_4Cl was readded back to bring the concentration to 2 mM when it fell below 1 mM. In order to fundamentally understand MP biotransformation capabilities of

DOI: 10.1021/acs.est.9b01037
Environ. Sci. Technol. 2019, 53, 8695−8705

each strain, cultures were incubated at their optimal growth temperatures for *N. inopinata* (42 °C), *N. gargensis* (46 °C), and *N. nitrosa* Nm90 (37 °C). First time point samples (0.5 mL) were taken immediately after biomass addition and then centrifuged at 16240 × *g* at 4 °C for 10 min; 0.3 mL of supernatant was transferred into 2 mL amber glass vials (with 300 μL-inserts), capped, and stored at 4 °C in dark until LC-HRMS/MS analysis (a maximum of 30 days of storage until analysis), while 0.1 mL of supernatant was transferred into 1.5 mL Eppendorf tubes and stored at −20 °C for further chemical measurements. The cell pellets were stored at −20 °C for total protein measurement. Subsequent samples were taken in the same way for *N. inopinata* at 18, 24, 48, 72, 96, 144, 240, and 336 h, *N. gargensis* at 4, 24, 48, 72, 96, 144, and 240 h, and *N. nitrosa* Nm90 at 16, 24, 48, 72, 94, 144, 240, 336, and 504 h. The incubation period is relevant to typical solid retention times (6−16 days) in suspended growth nitrifying reactors of WWTPs.[42]

Abiotic (without added biomass, with 4 g/L $CaCO_3$) and heat-inactivated biomass (121 °C and 103 kPa for 20 min) control experiments were set up in the same way as biotransformation experiments to examine the sorption potential of the selected micropollutants to the $CaCO_3$ precipitates in fresh medium and to the biomass, respectively, as well as the abiotic transformation potential at 46 °C (the highest temperature for cultivating the tested strains). For abiotic and heat-inactivated biomass controls, 2 mM ammonium and 6 mM nitrite were added (for *N. inopinata* controls, 6 mM nitrate was also added) to mimic the highest N levels in the biological samples and investigate possible abiotic transformation in the presence of ammonium, nitrite, and nitrate. Samples were taken at the same time points during the same incubation period as for the biotransformation experiments. In parallel, cultures amended with ammonium only (no micropollutant addition) were also set up as the positive control for ammonia oxidation activity. All experiments were performed in triplicates.

Biotransformation of Carbendazim by *N. inopinata*. To confirm the biotransformation of carbendazim by *N. inopinata*, the same biotransformation experiments were set up with an individual addition of carbendazim (40 μg/L) and were inoculated with 2−4 times concentrated biomass. To test whether the biotransformation of carbendazim by *N. inopinata* was associated with ammonia and/or nitrite oxidation, experiments were designed to provide *N. inopinata* with ammonium or nitrite as the sole energy source. Biotransformation experiments were set up using concentrated *N. inopinata* biomass under the following conditions: (1) 2 mM NH_4−N (with reamendment upon depletion to a total of 10 mM), with and without carbendazim; (2) 0.5 mM $NaNO_2$ (with reamendment upon depletion to a total of 2.5 mM) and 0.05 mM NH_4−N, with and without carbendazim; (3) 0.5 mM $NaNO_2$ (with reamendment upon depletion to a total of 2.5 mM), 0.05 mM NH_4−N, and 10 μM allylthiourea (ATU, a common AMO inhibitor resulting in a complete inhibition of ammonia oxidation at 10 μM), with and without carbendazim, and (4) 1 mM NH_4−N and 10 μM ATU (for ammonia oxidation inhibition control). We used 0.5 mM $NaNO_2$ as the accumulation of nitrite during complete ammonia oxidation by *N. inopinata* under these conditions can reach this level. We used ATU to inhibit comammox AMO by copper depletion rather than a mechanistic inhibitor specific to AOB such as octyne because the specificity of octyne to comammox AMO has not yet been investigated. Control experiments with heat-inactivated *N. inopinata* biomass were set up with the addition of 2 mM NH_4Cl, 0.5 mM $NaNO_2$, 6 mM $NaNO_3$, 10 μM ATU, and 40 μg/L carbendazim. Time series samples were taken over a 29 day incubation period. The two other ammonia oxidizers (*N. gargensis* and *N. nitrosa* Nm90) as well as the nitrite-oxidizing *N. defluvii* isolated from a WWTP[43] were tested with individual carbendazim compound addition for comparison. Cultures were amended with 2 mM NH_4−N and 2 mM NO_2−N (with reamendment back to 2 mM when below 1 mM) for ammonia-oxidizers and the nitrite-oxidizer, respectively. Samples were taken in time series over a 14 day incubation period.

Ammonium, Nitrite, and Nitrate Measurements. NH_4^+, NO_2^-, and NO_2^-/NO_3^- (NOx) concentrations were all measured colorimetrically. NH_4−N was measured by a colorimetric method.[44] Standards were prepared in the medium and ranged from 100 to 2000 μM NH_4Cl. Nitrite was measured using a sulfanilamide *N*-(1-naphthyl) ethylenediamine dihydrochloride (NED) reagent method.[45] Nitrate was reduced to nitrite by vanadium chloride and measured as NO_x by the Griess assay.[46] Standards were prepared in the medium and ranged from 100 to 2000 μM NO_x and from 100 to 2000 μM nitrite. All colorimetric analyses were performed using an Infinite 200 Pro spectrophotometer (Tecan Group AG, Männedorf, Switzerland).

Total Protein Measurement. Total protein was measured using a Pierce BCA Protein Assay Kit (Thermo Scientific, Regensburg, Germany) according to the manufacturer's instructions.

Estimation of Kinetic Parameters. To quantitatively compare biotransformation activities among biological samples, we estimated biotransformation rate constants (k_{bio}) normalized to total protein (Table S2) by using a first-order model described previously,[16] which incorporates abiotic sorption and transformation and biotransformation processes.[47,48] A Bayesian fitting procedure was used for parameter estimation as described elsewhere.[47] The median value calculated from the fitting procedure was used as the estimated k_{bio}, with the 5% and 95% percentile values representing the estimation uncertainty. The fitting quality was evaluated by plotting measured data against model predictions, including 90% credibility intervals and by the root-mean-square errors.

Analytical Method. Micropollutants, as well as their transformation products (TPs), were analyzed by liquid chromatography coupled to a high-resolution quadrupole-orbitrap mass spectrometer (LC- HRMS/MS) (Q Exactive, Thermo Fisher Scientific) as described previously.[40] In general, 50 μL sample was loaded onto a C_{18} Atlantis-T3 column (particle size 3 μm, 3.0 × 150 mm, Waters) and eluted at a flow rate of 350 μL/min with nanopure water (A) and acetonitrile (B) (both amended with 0.1% formic acid) at a gradient as follows: 5% B: 0−1 min, 5% − 100% B: 1−8 min, 100% B: 8−20 min, and 5% B: 20−26 min. Compounds in the eluate were measured in full scan mode on HRMS at a resolution of 70000 at m/z 200 and a scan range of m/z 50−750 in a positive/negative switching mode. The LC-HRMS full scan was used to measure parent compound concentrations and identify plausible transformation products (TPs). To elucidate TP structures, we measured the samples on LC-HRMS/MS for a second time, and data-dependent MS^2 using the exact masses of identified TPs was triggered after each full scan with a resolution of 17500 at 200 m/z at a normalized collision energy of 40. Dynamic exclusion technology was used to capture MS^2 spectra of each TP accurately.

DOI: 10.1021/acs.est.9b01037
Environ. Sci. Technol. 2019, 53, 8695−8705

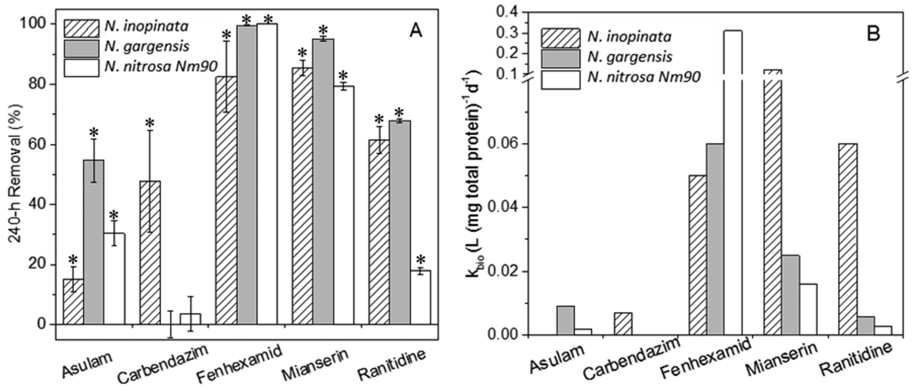

Figure 1. (A) Micropollutants biotransformed by *Nitrososphara gargensis* (AOA), *Nitrosomonas nitrosa* Nm90 (AOB), and *Nitrospira inopinata* (comammox) (n = 3, * indicates a statistically significant difference from the abiotic and heat-inactivated biomass controls, $p < 0.05$). (B) Biomass-normalized biotransformation rate constants, k_{bio} (bars represent the median k_{bio} values calculated based on a first-order model and a Bayesian fitting procedure, taking into account the adsorption and abiotic transformation; see Table S2 for complete results of simulated rate constants; k_{bio} of mianserin and ranitidine biotransformation by *N. gargensis* and *N. nitrosa* Nm90 was adopted from Men et al., 2016[16]).

Cell Extraction for Intracellular Micropollutant Concentration Measurement. A cell extraction procedure from a previous study[49] was adopted with slight modification. Briefly, internal standards were spiked in cell pellets collected from 10 mL of culture (at a final concentration of 4 μg/L for each) followed by an addition of 2 mL of lysis solvent containing methanol (0.5% formic acid)/nanopure water (0.1% w/w EDTA), 50:50 (v/v). The cells were disrupted by ultrasonication at 50 °C for 15 min and centrifuged at 8000 × g for 10 min. The supernatant was collected in a glass vial. This procedure was repeated for two more times for a better recovery. Finally, ~6 mL supernatant was evaporated to dryness under a gentle steam of dinitrogen gas at 40 °C. The analytes were redissolved in 0.5 mL of filter-sterilized fresh medium without $CaCO_3$; this mixture was then centrifuged at 8000 × g at 4 °C for 10 min. The supernatant was collected for LC-HRMS measurement.

Transformation Product (TP) Identification. As described in previous studies,[16,40,50] both suspect screening and nontarget screening were carried out to identify TPs. Generally, suspect screening was performed by TraceFinder 4.1 EFS software (Thermo Scientific). TP suspect lists were compiled using an automated metabolite mass prediction script, which considered a number of known redox and hydrolysis reactions as well as several conjugation reactions at primary and secondary levels. Plausible TPs were identified according to the following criteria: (i) isotopic pattern score > 70%; (ii) peak area > 5 × 10^6; (iii) increasing trend over time or an increase followed by a decrease; (iv) absent or at lower levels in biological samples without micropollutant addition and in heat-inactivated controls. Sieve 2.2 software (Thermos Scientific) was used for nontarget screening, and the TP candidates were selected based on the same criteria. MS^2 fragment profiles of TP candidates obtained using data-dependent MS/MS scan were used to elucidate TP structures. MarvinSketch (NET6.2.0, 2014) was used for drawing, displaying, and characterizing chemical structures (ChemAxon, http://www.chemaxon.com).

RESULTS AND DISCUSSION

Micropollutant Biotransformation by *N. inopinata*. First of all, we tested for absorption of the selected micropollutants to $CaCO_3$ precipitates and for abiotic transformation in the commonly used basal medium[38] containing ammonium, nitrite, and nitrate at the highest possible concentrations as those in the biological samples. MP abiotic transformation tests were performed at the highest incubation temperature (46 °C), and we assumed absence or lower abiotic transformation rates at lower temperatures. No more than 20% abiotic removal was observed for 15 of the 17 tested compounds (data not shown). Indomethacin was almost completely transformed abiotically after 120 h and was excluded from further analysis. Fenhexamid exhibited a 36% removal after 94 h and 86% after 504 h (Figure S1). Heat-inactivated biomass was used for testing the absorption of micropollutants on inactivated cells. No obvious micropollutant removal (>20%) was observed over a 94 h incubation. With a prolonged incubation of 504 h, fenhexamid in the heat-inactivated AOB culture showed a removal of 62% (Figure S1). These results indicate that except indomethacin and fenhexamid, all the other tested micropollutants did not adsorb on $CaCO_3$ precipitates or inactivated biomass or exhibit abiotic transformation after at least 240 h of incubation (for selected data see Figure S1). The abiotic transformation of fenhexamid after 94 h was not through nitration observed for other micropollutants,[51] as no corresponding transformation products were detected. Moreover, fenhexamid likely adsorbed on $CaCO_3$. The higher removal of fenhexamid in the medium control than in the heat-inactivated control containing the same amount of $CaCO_3$ precipitates (4 g/L) could indicate that the surface of the $CaCO_3$ particles was occupied by dead cells in the heat-inactivated control, resulting in reduced absorption of fenhexamid. In addition, at a concentration of 20 μg/L, the tested micropollutant mixtures (Table S1) exhibited no inhibitory effects on ammonia oxidation by the three ammonia oxidizers or nitrite oxidation by *N. inopinata* (Figure S2).

Five of the 17 tested micropollutants, i.e., asulam, carbendazim, fenhexamid, mianserin, and ranitidine showed biotransformation by *N. inopinata*. Except for asulam, which was only slightly biotransformed by 16%, the other four compounds exhibited 45−85% removals during the 240 h incubation period (Figures 1A and S1). For the tested AOA and AOB strains, a similar compound specificity was observed. These strains biotransformed asulam, fenhexamid, mianserin, and ranitidine, although at various biomass-normalized rates (Table S2, Figure 1B). Among the tested micropollutants, these four compounds were also previously reported by us to be biotransformed by another AOB strain (*N. europaea*). In addition. *N. europaea* also

DOI: 10.1021/acs.est.9b01037
Environ. Sci. Technol. 2019, 53, 8695−8705

transformed rufinamide and benzafibrate but at relatively lower removals than the other four compounds.[40] For asulam, *N. gargensis* exhibited the highest biotransformation rate among the three ammonia oxidizers, about 5 times higher than that of *N. nitrosa* Nm 90, while for biotransformation of fenhexamid, *N. nitrosa* Nm90 was the most efficient strain with a 5 times higher biotransformation rate than those of *N. inopinata* and *N. gargensis* (Figure 1B). The two pharmaceuticals, mianserin and ranitidine, which were demonstrated to be biotransformed by *N. gargensis* and *N. nitrosa* Nm 90,[16] were also biotransformed by *N. inopinata* with 240 h removals of 87% and 73%, respectively (Figure 1A, Table S2). Compared to AOA (*N. gargensis*) and AOB (*N. nitrosa* Nm90), respectively, the biotransformation rate constants of *N. inopinata* were 6 and 8 times higher for mianserin and 8 and 22 times higher for ranitidine. In addition, the previously identified TPs of mianserin, ranitidine, and asulam during biotransformation by the AOA and AOB species[16,40] were also detected during biotransformation by *N. inopinata* (Figure S3). All these TPs were formed via oxidation reactions that might be carried out by AMO,[16] which indicates that *N. inopinata* also likely converted mianserin and ranitidine via the same mechanism by AMO.

Surprisingly, and different from the above four micropollutants, carbendazim was biotransformed only by *N. inopinata* with a 240 h removal of 48% (Figure 1A). The biotransformation rate of carbendazim by *N. inopinata* was 8−17 times lower than those of fenhexamid, mianserin, and ranitidine. Moreover, according to our previous study, carbendazim cannot be transformed by either hydroxylamine or nitric oxide, which is different from the other four biotransformed compounds that underwent both cometabolic biotransformation by bacterial AMO and abiotic biotransformation mediated by ammonia oxidation intermediates.[40] It was previously hypothesized that the higher affinity of the archaeal AMO for the cometabolic substrate lead to a higher rate of micropollutant biotransformation by the AOA *N. gargensis* than by the AOB *N. nitrosa* Nm90.[16] Thus, the exclusive biotransformation of carbendazim by *N. inopinata* and its higher biotransformation rates of mianserin and ranitidine are also likely attributed to its phylogenetically different AMO and the remarkably high affinity of this enzyme.[35] In addition, *N. inopinata* excretes much more hydroxylamine than *N. gargensis* and *N. nitrosa* Nm90 during ammonia oxidation in batch culture with an initial ammonium concentration of 2 mM,[52] which will result in higher hydroxylamine-mediated abiotic transformation for the four compounds that can react with hydroxylamine (except for carbendazim).[40] The lower biotransformation rate of asulam by *N. inopinata* compared to the other tested ammonia-oxidizers suggests that AMO affinities vary among micropollutants. It is worth noting that carbendazim is structurally different from asulam and the other three biotransformed compounds as it contains a benzimidazole group. Thus, future studies should include more benzimidazole compounds to test whether compounds within this group are more generally biotransformed by *N. inopinata*.

Notably, besides AMO that is encoded by all known aerobic ammonia oxidizers, *N. inopinata* possesses a nitrite oxidoreductase (NXR), which enables its additional nitrite oxidation activity compared to AOB and AOA.[30] Although a previous study has demonstrated that the nitrite-oxidizing bacterium (NOB) *Nitrobacter* sp. was not able to biotransform any of the micropollutants investigated in this study,[40] it remains to be demonstrated whether the NXR enzyme of *N. inopinata*, that is significantly different than that of *Nitrobacter* NOB,[30,41] is contributing to the observed biotransformation reactions.

Mechanisms of Carbendazim Biotransformation by *N. inopinata*. We first confirmed the biotransformation of carbendazim in the absence of the other micropollutants by *N. inopinata* using an individual addition of carbendazim to the three investigated ammonia oxidizers. Consistent with the mixed micropollutant addition, among the three tested nitrifiers, only *N. inopinata* was able to biotransform carbendazim (Figure 2, Figure S4). To further confirm the enzymes involved in carbendazim biotransformation and elucidate the underlying mechanisms, we investigated carbendazim biotransformation activities by *N. inopinata* cells under various conditions: (1) ammonium as the energy source (2 mM with reamendment upon depletion to a total of ∼10 mM), where both AMO-involved ammonia oxidation and NXR-mediated nitrite

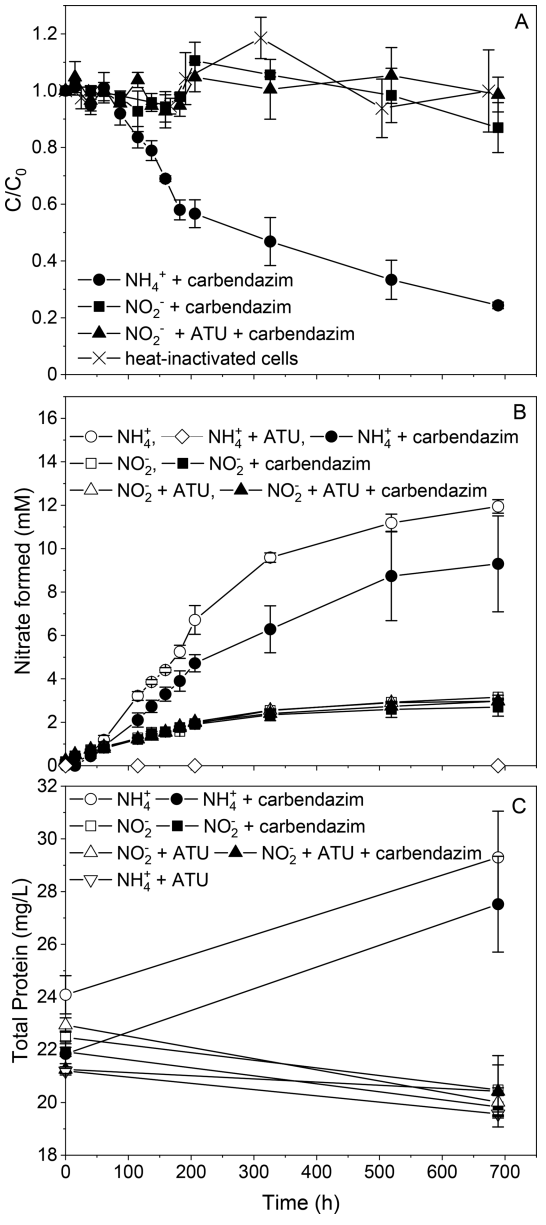

Figure 2. Carbendazim biotransformation (A), nitrate production (B), and cell growth measured as total protein (C) of *N. inopinata* under different growth conditions (n = 3).

DOI: 10.1021/acs.est.9b01037
Environ. Sci. Technol. 2019, 53, 8695−8705

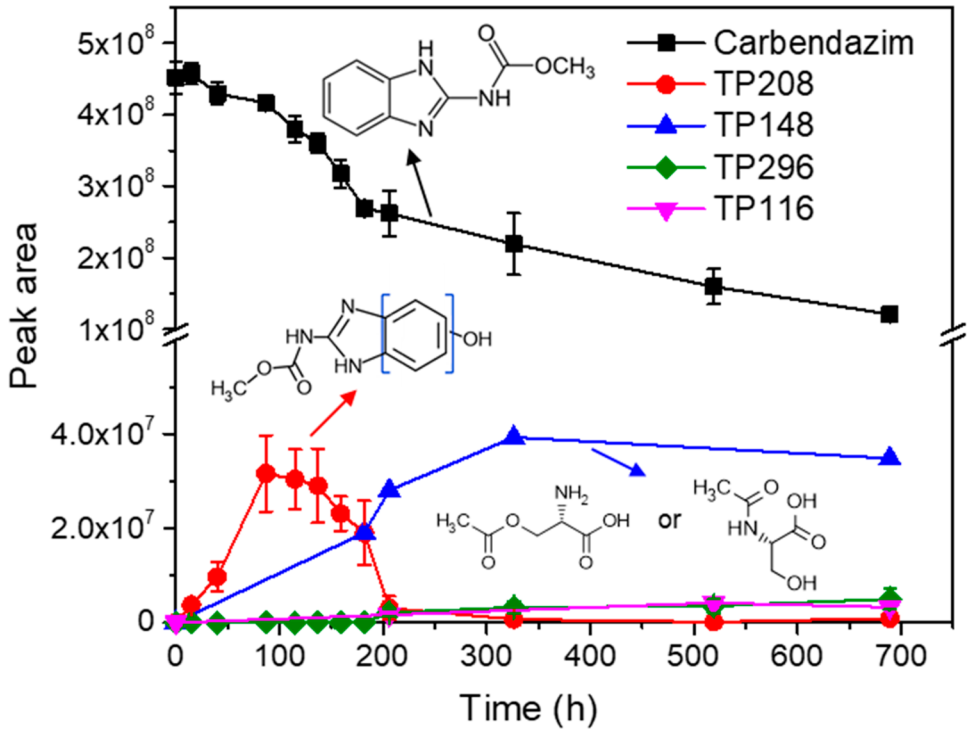

Figure 3. Carbendazim biotransformation and TP formation by *N. inopinata* (n = 3; note: for TP148 and TP116, the values represent the averaged peak areas in *N. inopinata* with carbendazim addition subtracted by the averaged peak areas in *N. inopinata* without carbendazim addition, representing the net formation of the two compounds).

oxidation were active; (2) nitrite as the energy source (0.5 mM with reamendment upon depletion to a total of ~2.5 mM), where NXR was active while the activity of enzymes involved in ammonia oxidation was suspended due to the lack of ammonium; (3) nitrite as the energy source with the same additions as in conditions in part 2 but with an AMO inhibitor (ATU), where NXR was active, and the activity of AMO was completely inhibited. When using nitrite as the energy source, we still added a small amount of ammonium (0.05 mM) as a nitrogen source, as *N. inopinata* cannot assimilate nitrite.[30] To eliminate potential AMO activity by oxidizing the added trace amount of ammonium for energy conversion, the commonly used AMO inhibitor ATU[53] was used. The inhibitory effect of ATU was confirmed as no nitrate formation was observed in *N. inopinata* grown on 1 mM ammonium in the presence of 10 μM (ca. 1.16 mg/L) ATU (Figure 2B). In all experiments, only the ammonium-amended *N. inopinata* culture biotransformed carbendazim with a 206 h removal of 57%, whereas nitrite-amended *N. inopinata* did not show any carbendazim biotransformation (Figure 2A).

All added ammonium/nitrite was completely converted by *N. inopinata* to nitrate (final product) in the absence of ATU. Ammonia oxidation was totally inhibited by the added ATU which did not affect nitrite oxidation. The maximum nitrate production rate from ammonium was slightly smaller with carbendazim addition than without (Figure 2B). This difference was due to either a slight inhibitory effect of carbendazim or the lower initial biomass of *N. inopinata* in the experiments with carbendazim addition (Figure 2C). A sustained activity of NXR and an overall metabolic activity of *N. inopinata* was indicated by the continuous oxidation of nitrite to nitrate in *N. inopinata* cells when nitrite was provided as the sole energy source with or without ATU addition. However, carbendazim biotransformation activity was lost in *N. inopinata* with nitrite (with or without ATU addition) (Figure 2A), suggesting that the biotransformation of carbendazim by *N. inopinata* was associated with ammonia oxidation rather than NXR-mediated nitrite oxidation. Even in *N. inopinata* fed with ammonia, there was a lag phase of ~100 h before carbendazim was actively biotransformed (Figures 2A and 3). This suggests that the biotransformation of carbendazim was via a cometabolic mechanism by AMO in which the conversion of carbendazim by AMO is mechanistically possible only when ammonia is present and ammonia oxidation is actively occurring. It is also worth noting that no growth of *N. inopinata* on nitrite was observed irrespective of the addition of ATU, despite the sustained catabolic activity and the presence of a small amount of ammonia (0.05 mM) for N-assimilation (Figure 2C). The reason for the inability of *N. inopinata* to grow on nitrite in the presence of a suitable nitrogen source remained unknown; one possible reason was insufficient reducing power (ammonia) for carbon fixation with and without ATU, as *N. inopinata* lacks the pathway to generate reducing power from nitrite to quinone via the reverse electron transport for carbon fixation.[30]

We also tested carbendazim biotransformation by a (non-ammonia-oxidizing) nitrite-oxidizing bacterium *N. defluvii*,[41,43] which is phylogenetically related to *N. inopinata*. Within a 14 d incubation, *N. defluvii* showed no carbendazim biotransformation activity (Figure S4). This corroborates the observation that enzymes involved in the nitrite-oxidizing metabolic pathway did not contribute to the biotransformation of carbendazim.

Carbendazim Transformation Product (TP) Identification. TPs of carbendazim biotransformation by *N. inopinata* were analyzed to understand the biotransformation pathways and mechanisms. According to the suspect and nontarget screening results, four tentative TPs (Figure 3) with m/z values

DOI: 10.1021/acs.est.9b01037
Environ. Sci. Technol. 2019, 53, 8695−8705

of 208.0713 ($[M + H]^+$, denoted TP208), 296.0273 ($[M - H]^-$, denoted TP296), 148.0601 ($[M + H]^+$, denoted TP148), and 116.0492 ($[M - H]^-$, denoted TP116) were identified according to the screening criteria. The confidence level of structure elucidation for each TP was assigned based on the criteria set up by Schymanski et al.[54]

TP208 and TP148 were the two dominant ones during carbendazim biotransformation by *N. inopinata* over ~29 d. TP208 was the most plausible TP based on the structure elucidation. The MS^2 fragments of TP208 all revealed an intact aromatic ring with an oxygen element, indicating that TP208 was a hydroxylation product of carbendazim with the addition of −OH group on the aromatic ring (confidence level 2b) (Figure 4). Such hydroxylation reactions are typically carried out by

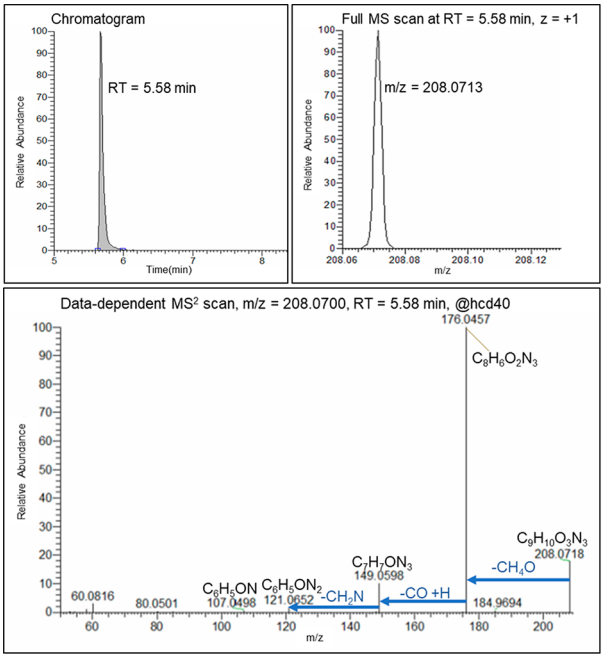

Formula: $C_9H_9O_3N_3$ **Atomic Modification:** +O

Hypothetical Structure: **Confidence level:** 2b

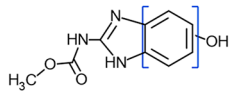

Figure 4. Carbendazim TP208 structure elucidation.

AMO.[21] Thus, consistent with the above result that carbendazim biotransformation only occurred in *N. inopinata* grown on ammonia, AMO is highly likely the responsible enzyme initiating carbendazim biotransformation. TP208 was accumulated during the first 96 h and then decreased and disappeared, suggesting secondary biotransformation to other TPs (Figure 3).

MS^2 fragments of TP148 revealed the same MS^2 fragmentation profile as *O*-acetyl-L-serine ($C_5H_9O_4N$) deposited in the MassBank MS^2 library (MassBank Accession: PR100272) (https://massbank.eu). We further obtained the MS^2 spectra of *O*-acetyl-L-serine using the authentic standard as well as the MS^2 spectra of its isomer *N*-acetyl-L-serine, both of which matched with the MS^2 spectra of TP148 at the same retention times (RTs) (Figure S5). Thus, we identified TP148 as acetyl-L-serine (confidence level 1) in general without differentiating proportions of the two isomers. The sums of peak areas at the two RTs were used to analyze the formation of TP148. *O*-acetyl-L-serine is an intermediate of cysteine biosynthesis in bacteria. In line with that, TP148 was detected in *N. inopinata* grown on ammonium without the addition of carbendazim. Moreover, TP148 was only detected in *N. inopinata* with ammonia addition but not with nitrite addition (nitrite does not support *N. inopinata* growth) or in the medium of the other two AOA and AOB species grown on ammonia. This indicates that TP148 was exclusively excreted by actively growing *N. inopinata* cells. The efflux of metabolites of the cysteine biosynthesis pathway, including *O*- and *N*-acetyl-L-serine, was observed in *Escherichia coli* by a facilitator protein.[55] *N. inopinata* might possess similar facilitator proteins for the excretion of acetyl-L-serine. Interestingly, TP148 (acetyl-L-serine) was identified by the nontarget screening as a tentative TP because its abundance was more than doubled with the addition of carbendazim in *N. inopinata* cultures (Figure S6A). However, as no plausible biotransformation pathway from carbendazim to acetyl-L-serine can be inferred based on the present data, we are unable to verify whether acetyl-L-serine was a true TP of carbendazim or not. More likely, acetyl-L-serine was overproduced and/or excreted by *N. inopinata* when exposed to carbendazim for unknown reasons.

The other two minor TPs (peak area $<10^7$), i.e., TP296 ($C_9H_7O_7N_5$) and TP116 only showed up after about 8 days (Figure 3), suggesting that they were secondary TPs. TP296 was likely formed by the addition of two nitro groups and one −OH group to the aromatic ring (Figure S7), whereas the formula and the structure of TP116 remain elusive (confidence level 5) as the exact mass does not give a plausible formula within the mass tolerance threshold (5 ppm), and the MS^2 profile does not provide sufficient information for an unambiguous structure (Figure S8). Like TP148, TP116 was also a metabolic intermediate of *N. inopinata*, which was detected in *N. inopinata* without carbendazim addition but at lower levels than in carbendazim biotransformation samples (Figure S6B). Thus, the additional amount of TP116 in *N. inopinata* with carbendazim addition could also be due to the stimulated formation/excretion in the presence of carbendazim for unknown reasons. The benzimidazole functional group in carbendazim was altered or lost in all proposed TPs, which can result in decreased or lost fungicidal activities, thus leading to less toxicity.

To examine active uptake by living cells, we further analyzed the intracellular occurrence of carbendazim and the detected TPs in extracts of washed cells collected at the end of the incubation using suspect and nontarget screening based on the same screening criteria. No carbendazim or TP was detected, suggesting no active uptake or accumulation of carbendazim or TPs in the living cells. As the reference compounds were not available for all TPs, we used peak areas to estimate the mass balance by assuming the parent compounds and the TPs have the same ionization efficiency on LC-HRMS.[50] We observed an incomplete mass balance (~45% recovery) of carbendazim. This could be due to the formation of smaller or nonionizable TPs undetectable by the current LC-HRMS method or due to the inaccurate estimation of concentrations based on peak areas without taking into account the different ionization efficiencies in positive (for carbendazim, TP 208 and TP148) and negative (for TP296 and TP116) ionization modes. If ring-cleavage biotransformation was occurring, carbendazim could also be

DOI: 10.1021/acs.est.9b01037
Environ. Sci. Technol. 2019, 53, 8695−8705

partially assimilated into the biomass or be mineralized to carbon dioxide.

Environmental Relevance. Comammox represents a group of nitrifiers that have been previously overlooked. They possess physiological characters distinct from the other common ammonia and nitrite oxidizers and may play important yet understudied ecological roles in natural and engineered environments. Therefore, in this study, we explored their contributions to the environmental fate of micropollutants. The comammox isolate *N. inopinata* was the only one among the three tested ammonia oxidizers that can biotransform carbendazim, a benzimidazole fungicide widely used over the past decades and frequently detected in wastewater, groundwater, and surface water.[56−62] In the environment, carbendazim is very stable and relatively persistent.[63−65] A few isolated bacteria are able to mineralize or degrade carbendazim as the sole nitrogen and carbon source.[66−70] The identified common pathway of carbendazim degradation by those bacteria starts with carbendazim hydrolysis, forming 2-aminobenzimidazole, which was further converted to 2-hydroxybenzimidazole, 1,2-diaminobenzene, catechol, and then carbon dioxide.[68,70] Among the above-reported biotransformation intermediates, only 1,2-diaminobenzene was detected in this study at low levels, but it occurred in all experimental samples and controls. The peak areas in the heat-inactivated control were even higher than those in the biotransformation samples, indicating that its formation was due to abiotic rather than biological degradation of carbendazim. Different from the reported metabolic pathways, *N. inopinata* employed cometabolic pathways by oxidizing carbendazim into a hydroxylated TP first, which was further converted to other TPs different from the ones identified in carbendazim mineralization by other bacterial species. As comammox bacteria are found in various environments such as soil, sediments, freshwater, and WWTPs, they may make special contributions to carbendazim removal in those systems.

Mianserin is a widely used second-generation tetracyclic antidepressant,[71] and ranitidine is a highly used gastrointestinal drug which inhibits stomach acid production.[72,73] Both are detectable at ng/L levels in various environments.[72,74] In this study, *N. inopinata* is able to biotransform these two compounds, like previously tested AOA and AOB species.[16] Asulam is one of the most effective systemic herbicides for controlling the growth of a variety of bracken by inhibiting germination.[75,76] Fenhexamid (a dicarboximide) is a widespread fungicide that inhibits DNA and RNA synthesis and cell division in fungi.[77−79] Both asulam and fenhexamid are heavily used in agriculture. Here, we determined for the first time that all tested ammonia oxidizers have abilities to biotransform these two compounds, providing new clues for the fate of these two compounds in nitrifying agro-environments. To fundamentally understand the biotransformation capabilities of the different ammonia oxidizers, for each strain investigated, the biotransformation rate constants were calculated and compared at their optimal growth temperature. Ideally, the biotransformation rate constants should be corrected by the temperature correction factor (Q_{10} for a 10 °C temperature difference) to a typical temperature found in systems important for micropollutant biotransformation. Q_{10} is reaction- and culture/enzyme-specific, and various Q_{10} values (1−17.6) have been determined for AOA and AOB cultures.[80,81] However, as Q_{10} values between 20 °C and the optimal temperature for the investigated ammonia oxidizers are unknown, the actual temperature effects of MP biotransformation are uncertain. Decreased activities may be expected at a lower temperature. Nonetheless, for all five compounds, substantial removal (>20%) was reported in a nitrifying activated sludge community at room temperature, where ammonia oxidizers showed significant contribution to the transformation of these micropollutants.[8]

In summary, the discovery of comammox *Nitrospira* has fundamentally changed our view of nitrification.[30,31] In this study, we demonstrate that the comammox organism *N. inopinata* (the only comammox isolate available) is capable of biotransforming five micropollutants (including a compound not transformed by the tested AOA and AOB) suggesting that comammox should be considered as a player for micropollutant biotransformation, too. The distinct ecological niche of comammox due to its remarkably high substrate affinity and yield in comparison to AOA and AOB might add weight to the role of comammox bacteria in micropollutant biotransformation, especially in oligotrophic ecosystems where comammox bacteria are the dominant ammonia oxidizers.[35] Different removal percentages and rate constants of the tested micropollutants may be expected for other comammox bacteria with different origins than *N. inopinata*. The findings collectively expand our knowledge of micropollutant biotransformation by ammonia oxidizers and provide important fundamental insights into the potential fate of certain micropollutants in nitrifying environments colonized by different ammonia oxidizers.

■ ASSOCIATED CONTENT

Supporting Information

The Supporting Information is available free of charge on the ACS Publications website at DOI: 10.1021/acs.est.9b01037.

List of micropollutants investigated and their detection on LC-HRMS/MS; biomass-normalized first-order biotransformation rate constants; biotranformation curve; nitrite/nitrate production; TP formation of ranitidine and mianserin by *N. inopinata*; removal of carbendazim after individual addition (without the other micropollutants) by *N. gargensis*, *N. nitrosa* Nm90, and *N. defluvii* during ammonia/nitrite oxidation; full MS scan and MS^2 fragmentation profiles of *N*-acetyl-L-serine, *O*-acetyl-L-serine (B), and carbendazim TP148; formation of TP148 and TP116 in *N. inopinata* with and without carbendazim; full MS scan and MS^2 fragmentation profiles (PDF)

■ AUTHOR INFORMATION

Corresponding Author

*E-mail: ymen2@illinois.edu. Phone: +1 (217) 244-8259.

ORCID

Yaochun Yu: 0000-0001-9231-6026

Zhenyu Tian: 0000-0002-7491-7028

Yujie Men: 0000-0001-9811-3828

Author Contributions

$P. H. and Y. Y. contributed equally.

Notes

The authors declare no competing financial interest.

■ ACKNOWLEDGMENTS

We would like to thank the National Natural Science Foundation of China (41807465, 41725002, 31770551, 41730646, and 41761144062) and Chinese National Key Programs for Fundamental Research and Development (No. 2016YFA0600904). P.H. and M.W. were supported by the

DOI: 10.1021/acs.est.9b01037
Environ. Sci. Technol. 2019, 53, 8695−8705

European Research Council Advanced Grant Project NITRICARE 294343 and the Comammox Research Platform of the University of Vienna (MW). L.J.Z was supported by the National Science & Technology Pillar Program (2015BAD13B01). Q.L.W. was supported by Fifth Stage 333 High-level-talent Training Project of Jiangsu Province (BRA2017574).

REFERENCES

(1) Fenner, K.; Canonica, S.; Wackett, L. P.; Elsner, M. Evaluating pesticide degradation in the environment: blind spots and emerging opportunities. *Science* **2013**, *341*, 752−758.
(2) Schwarzenbach, R. P.; Escher, B. I.; Fenner, K.; Hofstetter, T. B.; Johnson, C. A.; von Gunten, U.; Wehrli, B. The challenge of micropollutants in aquatic systems. *Science* **2006**, *313*, 1072−1077.
(3) Luo, Y. L.; Guo, W. S.; Ngo, H. H.; Nghiem, L. D.; Hai, F. I.; Zhang, J.; Liang, S.; Wang, X. C. C. A review on the occurrence of micropollutants in the aquatic environment and their fate and removal during wastewater treatment. *Sci. Total Environ.* **2014**, *473*, 619−641.
(4) Margot, J.; Rossi, L.; Barry, D. A.; Holliger, C. A review of the fate of micropollutants in wastewater treatment plants. *Wiley Interdiscip. Rev.: Water* **2015**, *2*, 457−487.
(5) Helbling, D. E.; Johnson, D. R.; Honti, M.; Fenner, K. Micropollutant biotransformation kinetics associate with WWTP process parameters and microbial community characteristics. *Environ. Sci. Technol.* **2012**, *46*, 10579−10588.
(6) Tran, N. H.; Urase, T.; Ngo, H. H.; Hu, J. Y.; Ong, S. L. Insight into metabolic and cometabolic activities of autotrophic and heterotrophic microorganisms in the biodegradation of emerging trace organic contaminants. *Bioresour. Technol.* **2013**, *146*, 721−731.
(7) Xu, Y. F.; Yuan, Z. G.; Ni, B. J. Impact of Ammonium Availability on Atenolol Biotransformation during Nitrification. *ACS Sustainable Chem. Eng.* **2017**, *5*, 7137−7144.
(8) Men, Y.; Achermann, S.; Helbling, D. E.; Johnson, D. R.; Fenner, K. Relative contribution of ammonia-oxidizing bacteria and other members of nitrifying activated sludge communities to micropollutant biotransformation. *Water Res.* **2017**, *109*, 217−226.
(9) Li, F.; Jiang, B.; Nastold, P.; Kolvenbach, B. A.; Chen, J.; Wang, L.; Guo, H.; Corvini, P. F.; Ji, R. Enhanced transformation of tetrabromobisphenol a by nitrifiers in nitrifying activated sludge. *Environ. Sci. Technol.* **2015**, *49*, 4283−4292.
(10) Rattier, M.; Reungoat, J.; Keller, J.; Gernjak, W. Removal of micropollutants during tertiary wastewater treatment by biofiltration: role of nitrifiers and removal mechanisms. *Water Res.* **2014**, *54C*, 89−99.
(11) Fernandez-Fontaina, E.; Omil, F.; Lema, J. M.; Carballa, M. Influence of nitrifying conditions on the biodegradation and sorption of emerging micropollutants. *Water Res.* **2012**, *46*, 5434−5444.
(12) Khunjar, W. O.; Mackintosh, S. A.; Skotnicka-Pitak, J.; Baik, S.; Aga, D. S.; Love, N. G. Elucidating the relative roles of ammonia-oxidizing and heterotrophic bacteria during the biotransformation of 17alpha-Ethinylestradiol and Trimethoprim. *Environ. Sci. Technol.* **2011**, *45*, 3605−3612.
(13) Batt, A. L.; Kim, S.; Aga, D. S. Enhanced biodegradation of iopromide and trimethoprim in nitrifying activated sludge. *Environ. Sci. Technol.* **2006**, *40*, 7367−7373.
(14) Xing, Y.; Yu, Y. C.; Men, Y. J. Emerging investigators series: occurrence and fate of emerging organic contaminants in wastewater treatment plants with an enhanced nitrification step. *Environ. Sci-Wat. Res.* **2018**, *4*, 1412−1426.
(15) Xu, Y. F.; Yuan, Z. G.; Ni, B. J. Biotransformation of acyclovir by an enriched nitrifying culture. *Chemosphere* **2017**, *170*, 25−32.
(16) Men, Y.; Han, P.; Helbling, D. E.; Jehmlich, N.; Herbold, C.; Gulde, R.; Onnis-Hayden, A.; Gu, A. Z.; Johnson, D. R.; Wagner, M.; Fenner, K. Biotransformation of two pharmaceuticals by the ammonia-oxidizing archaeon *Nitrososphaera gargensis*. *Environ. Sci. Technol.* **2016**, *50*, 4682−4692.
(17) Gao, J. F.; Luo, X.; Wu, G. X.; Li, T.; Peng, Y. Z. Quantitative analyses of the composition and abundance of ammonia-oxidizing archaea and ammonia-oxidizing bacteria in eight full-scale biological wastewater treatment plants. *Bioresour. Technol.* **2013**, *138*, 285−296.
(18) Wells, G. F.; Park, H. D.; Yeung, C. H.; Eggleston, B.; Francis, C. A.; Criddle, C. S. Ammonia-oxidizing communities in a highly aerated full-scale activated sludge bioreactor: betaproteobacterial dynamics and low relative abundance of *Crenarchaea*. *Environ. Microbiol.* **2009**, *11*, 2310−2328.
(19) Mussmann, M.; Brito, I.; Pitcher, A.; Sinninghe Damste, J. S.; Hatzenpichler, R.; Richter, A.; Nielsen, J. L.; Nielsen, P. H.; Muller, A.; Daims, H.; Wagner, M.; Head, I. M. Thaumarchaeotes abundant in refinery nitrifying sludges express *amoA* but are not obligate autotrophic ammonia oxidizers. *Proc. Natl. Acad. Sci. U. S. A.* **2011**, *108*, 16771−16776.
(20) Kjeldal, H.; Pell, L.; Pommerening-Roser, A.; Nielsen, J. L. Influence of p-cresol on the proteome of the autotrophic nitrifying bacterium *Nitrosomonas eutropha* C91. *Arch. Microbiol.* **2014**, *196*, 497−511.
(21) Keener, W. K.; Arp, D. J. Transformations of aromatic compounds by *Nitrosomonas europaea*. *Appl. Environ. Microbiol.* **1994**, *60*, 1914−1920.
(22) Chang, S. W.; Hyman, M. R.; Williamson, K. J. Cooxidation of naphthalene and other polycyclic aromatic hydrocarbons by the nitrifying bacterium. *Biodegradation* **2002**, *13*, 373−381.
(23) Hooper, A. B.; Vannelli, T.; Bergmann, D. J.; Arciero, D. M. Enzymology of the oxidation of ammonia to nitrite by bacteria. *Antonie van Leeuwenhoek* **1997**, *71*, 59−67.
(24) Roh, H.; Subramanya, N.; Zhao, F.; Yu, C. P.; Sandt, J.; Chu, K. H. Biodegradation potential of wastewater micropollutants by ammonia-oxidizing bacteria. *Chemosphere* **2009**, *77*, 1084−1089.
(25) Shi, J.; Fujisawa, S.; Nakai, S.; Hosomi, M. Biodegradation of natural and synthetic estrogens by nitrifying activated sludge and ammonia-oxidizing bacterium *Nitrosomonas europaea*. *Water Res.* **2004**, *38*, 2322−2329.
(26) Sauder, L. A.; Albertsen, M.; Engel, K.; Schwarz, J.; Nielsen, P. H.; Wagner, M.; Neufeld, J. D. Cultivation and characterization of *Candidatus* Nitrosocosmicus exaquare, an ammonia-oxidizing archaeon from a municipal wastewater treatment system. *ISME J.* **2017**, *11*, 1142−1157.
(27) Zhang, T.; Jin, T.; Yan, Q.; Shao, M.; Wells, G.; Criddle, C.; P Fang, H.H. Occurrence of ammonia-oxidizing Archaea in activated sludges of a laboratory scale reactor and two wastewater treatment plants. *J. Appl. Microbiol.* **2009**, *107*, 970−977.
(28) Li, Y.; Ding, K.; Wen, X.; Zhang, B.; Shen, B.; Yang, Y. A novel ammonia-oxidizing archaeon from wastewater treatment plant: its enrichment, physiological and genomic characteristics. *Sci. Rep.* **2016**, *6*, 23747.
(29) Pornkulwat, P.; Kurisu, F.; Soonglerdsongpha, S.; Banjongproo, P.; Srithep, P.; Limpiyakorn, T. Incorporation of ^{13}C-HCO_3^- by ammonia-oxidizing archaea and bacteria during ammonia oxidation of sludge from a municipal wastewater treatment plant. *Appl. Microbiol. Biotechnol.* **2018**, *102*, 10767−10777.
(30) Daims, H.; Lebedeva, E. V.; Pjevac, P.; Han, P.; Herbold, C.; Albertsen, M.; Jehmlich, N.; Palatinszky, M.; Vierheilig, J.; Bulaev, A.; Kirkegaard, R. H.; von Bergen, M.; Rattei, T.; Bendinger, B.; Nielsen, P. H.; Wagner, M. Complete nitrification by *Nitrospira* bacteria. *Nature* **2015**, *528*, 504−509.
(31) van Kessel, M. A.; Speth, D. R.; Albertsen, M.; Nielsen, P. H.; Op den Camp, H. J.; Kartal, B.; Jetten, M. S.; Lücker, S. Complete nitrification by a single microorganism. *Nature* **2015**, *528*, 555−559.
(32) Zheng, M.; Wang, M.; Zhao, Z.; Zhou, N.; He, S.; Liu, S.; Wang, J.; Wang, X. Transcriptional activity and diversity of comammox bacteria as a previously overlooked ammonia oxidizing prokaryote in full-scale wastewater treatment plants. *Sci. Total Environ.* **2019**, *656*, 717−722.
(33) Wang, M.; Huang, G.; Zhao, Z.; Dang, C.; Liu, W.; Zheng, M. Newly designed primer pair revealed dominant and diverse comammox

DOI: 10.1021/acs.est.9b01037
Environ. Sci. Technol. 2019, 53, 8695−8705

amoA gene in full-scale wastewater treatment plants. *Bioresour. Technol.* **2018**, *270*, 580−587.
(34) Pjevac, P.; Schauberger, C.; Poghosyan, L.; Herbold, C. W.; van Kessel, M.; Daebeler, A.; Steinberger, M.; Jetten, M. S. M.; Lücker, S.; Wagner, M.; Daims, H. *AmoA*-targeted polymerase chain reaction primers for the specific detection and quantification of comammox Nitrospira in the environment. *Front. Microbiol.* **2017**, *8*, 1508.
(35) Kits, K. D.; Sedlacek, C. J.; Lebedeva, E. V.; Han, P.; Bulaev, A.; Pjevac, P.; Daebeler, A.; Romano, S.; Albertsen, M.; Stein, L. Y.; Daims, H.; Wagner, M. Kinetic analysis of a complete nitrifier reveals an oligotrophic lifestyle. *Nature* **2017**, *549*, 269−272.
(36) Zhou, L. J.; Han, P.; Yu, Y.; Wang, B.; Men, Y.; Wagner, M.; Wu, Q. L. Cometabolic biotransformation and microbial-mediated abiotic transformation of sulfonamides by three ammonia oxidizers. *Water Res.* **2019**, *159*, 444−453.
(37) Koops, H. P.; Bottcher, B.; Moller, U. C.; Pommerening-Roser, A.; Stehr, G. Classification of eight new species of ammonia-oxidizing bacteria: *Nitrosomonas communis* sp. nov., *Nitrosomonas ureae* sp. nov., *Nitrosomonas aestuarii* sp. nov., *Nitrosomonas marina* sp. nova, *Nitrosomonas nitrosa* sp. nov., *Nitrosomonas eutropha* sp. nov., *Nitrosomonas oligotropha* spa nov. and *Nitrosomonas halophila* sp. nova. *J. Gen. Microbiol.* **1991**, *137*, 1689−1699.
(38) Palatinszky, M.; Herbold, C.; Jehmlich, N.; Pogoda, M.; Han, P.; von Bergen, M.; Lagkouvardos, I.; Karst, S. M.; Galushko, A.; Koch, H.; Berry, D.; Daims, H.; Wagner, M. Cyanate as an energy source for nitrifiers. *Nature* **2015**, *524*, 105−108.
(39) Hatzenpichler, R.; Lebedeva, E. V.; Spieck, E.; Stoecker, K.; Richter, A.; Daims, H.; Wagner, M. A moderately thermophilic ammonia-oxidizing crenarchaeote from a hot spring. *Proc. Natl. Acad. Sci. U. S. A.* **2008**, *105*, 2134−2139.
(40) Yu, Y.; Han, P.; Zhou, L. J.; Li, Z.; Wagner, M.; Men, Y. Ammonia monooxygenase-mediated cometabolic biotransformation and hydroxylamine-mediated abiotic transformation of micropollutants in an AOB/NOB coculture. *Environ. Sci. Technol.* **2018**, *52*, 9196−9205.
(41) Lücker, S.; Wagner, M.; Maixner, F.; Pelletier, E.; Koch, H.; Vacherie, B.; Rattei, T.; Damsté, J. S.; Spieck, E.; Le Paslier, D.; Daims, H. A *Nitrospira* metagenome illuminates the physiology and evolution of globally important nitrite-oxidizing bacteria. *Proc. Natl. Acad. Sci. U. S. A.* **2010**, *107*, 13479−13484.
(42) Mara, D.; Horan, N. *Handbook of water and wastewater microbiology*. Academic Press: 2003.
(43) Spieck, E.; Hartwig, C.; McCormack, I.; Maixner, F.; Wagner, M.; Lipski, A.; Daims, H. Selective enrichment and molecular characterization of a previously uncultured *Nitrospira*-like bacterium from activated sludge. *Environ. Microbiol.* **2006**, *8*, 405−415.
(44) Kandeler, E.; Gerber, H. Short-term assay of soil urease activity using colorimetric determination of ammonium. *Biol. Fertil. Soils* **1988**, *6*, 68−72.
(45) Griess-Romijn van Eck, E. Physiological and chemical tests for drinking water. 1966.
(46) Miranda, K. M.; Espey, M. G.; Wink, D. A. A rapid, simple spectrophotometric method for simultaneous detection of nitrate and nitrite. *Nitric Oxide* **2001**, *5*, 62−71.
(47) Gulde, R.; Helbling, D. E.; Scheidegger, A.; Fenner, K. pH-dependent biotransformation of ionizable organic micropollutants in activated sludge. *Environ. Sci. Technol.* **2014**, *48*, 13760−13768.
(48) Helbling, D. E.; Hollender, J.; Kohler, H. P.; Fenner, K. Structure-based interpretation of biotransformation pathways of amide-containing compounds in sludge-seeded bioreactors. *Environ. Sci. Technol.* **2010**, *44*, 6628−6635.
(49) Gago-Ferrero, P.; Borova, V.; Dasenaki, M. E.; Thomaidis, Ni. S. Simultaneous determination of 148 pharmaceuticals and illicit drugs in sewage sludge based on ultrasound-assisted extraction and liquid chromatography-tandem mass spectrometry. *Anal. Bioanal. Chem.* **2015**, *407*, 4287−4297.
(50) Gulde, R.; Meier, U.; Schymanski, E. L.; Kohler, H. P.; Helbling, D. E.; Derrer, S.; Rentsch, D.; Fenner, K. Systematic exploration of biotransformation reactions of amine-containing micropollutants in activated sludge. *Environ. Sci. Technol.* **2016**, *50*, 2908−2920.
(51) Sun, Q.; Li, Y.; Chou, P. H.; Peng, P. Y.; Yu, C. P. Transformation of bisphenol A and alkylphenols by ammonia-oxidizing bacteria through nitration. *Environ. Sci. Technol.* **2012**, *46*, 4442−4448.
(52) Liu, S.; Han, P.; Hink, L.; Prosser, J. I.; Wagner, M.; Bruggemann, N. Abiotic conversion of extracellular NH_2OH contributes to N_2O emission during ammonia oxidation. *Environ. Sci. Technol.* **2017**, *51*, 13122−13132.
(53) Guellil, A.; Block, J.-C.; Urbain, V. Estimation of nitrifying bacterial activities by measuring oxygen uptake in the presence of the metabolic inhibitors allylthiourea and azide. *Water Sci. Technol.* **1998**, *64*, 2266−2268.
(54) Schymanski, E. L.; Jeon, J.; Gulde, R.; Fenner, K.; Ruff, M.; Singer, H. P.; Hollender, J. Identifying small molecules via high resolution mass spectrometry: communicating confidence. *Environ. Sci. Technol.* **2014**, *48*, 2097−2098.
(55) Dassler, T.; Maier, T.; Winterhalter, C.; Bock, A. Identification of a major facilitator protein from *Escherichia coli* involved in efflux of metabolites of the cysteine pathway. *Mol. Microbiol.* **2000**, *36*, 1101−1112.
(56) Salunkhe, V. P.; Sawant, I. S.; Banerjee, K.; Wadkar, P. N.; Sawant, S. D.; Hingmire, S. A. Kinetics of degradation of carbendazim by B. subtilis strains: possibility of in situ detoxification. *Environ. Monit. Assess.* **2014**, *186*, 8599−8610.
(57) Huntscha, S.; Singer, H. P.; McArdell, C. S.; Frank, C. E.; Hollender, J. Multiresidue analysis of 88 polar organic micropollutants in ground, surface and wastewater using online mixed-bed multilayer solid-phase extraction coupled to high performance liquid chromatography-tandem mass spectrometry. *J. Chromatogr. A* **2012**, *1268*, 74−83.
(58) Singer, H.; Jaus, S.; Hanke, I.; Luck, A.; Hollender, J.; Alder, A. C. Determination of biocides and pesticides by on-line solid phase extraction coupled with mass spectrometry and their behaviour in wastewater and surface water. *Environ. Pollut.* **2010**, *158*, 3054−3064.
(59) Margot, J.; Kienle, C.; Magnet, A.; Weil, M.; Rossi, L.; de Alencastro, L. F.; Abegglen, C.; Thonney, D.; Chevre, N.; Scharer, M.; Barry, D. A. Treatment of micropollutants in municipal wastewater: ozone or powdered activated carbon? *Sci. Total Environ.* **2013**, *461*−*462*, 480−498.
(60) Hollender, J.; Zimmermann, S. G.; Koepke, S.; Krauss, M.; McArdell, C. S.; Ort, C.; Singer, H.; von Gunten, U.; Siegrist, H. Elimination of organic micropollutants in a municipal wastewater treatment plant upgraded with a full-scale post-ozonation followed by sand filtration. *Environ. Sci. Technol.* **2009**, *43*, 7862−7869.
(61) Merel, S.; Benzing, S.; Gleiser, C.; Di Napoli-Davis, G.; Zwiener, C. Occurrence and overlooked sources of the biocide carbendazim in wastewater and surface water. *Environ. Pollut.* **2018**, *239*, 512−521.
(62) Bollmann, U. E.; Tang, C.; Eriksson, E.; Jonsson, K.; Vollertsen, J.; Bester, K. Biocides in urban wastewater treatment plant influent at dry and wet weather: concentrations, mass flows and possible sources. *Water Res.* **2014**, *60*, 64−74.
(63) Kiigemagi, U.; Inman, R. D.; Mellenthin, W. M.; Deinzer, M. L. Residues of benomyl (determined as carbendazim) and captan in postharvest-treated pears in cold-storage. *J. Agric. Food Chem.* **1991**, *39*, 400−403.
(64) Thapar, S.; Bhushan, R.; Mathur, R. P. Degradation of organophosphorus and carbamate pesticides in soils - HPLC determination. *Biomed. Chromatogr.* **1995**, *9*, 18−22.
(65) Van den Brink, P. J.; Hattink, J.; Bransen, F.; Van Donk, E.; Brock, T. C. M. Impact of the fungicide carbendazim in freshwater microcosms. II. Zooplankton, primary producers and final conclusions. *Aquat. Toxicol.* **2000**, *48*, 251−264.
(66) Pandey, G.; Dorrian, S. J.; Russell, R. J.; Brearley, C.; Kotsonis, S.; Oakeshott, J. G. Cloning and biochemical characterization of a novel carbendazim (methyl-1*H*-benzimidazol-2-ylcarbamate)-hydrolyzing esterase from the newly isolated *Nocardioides* sp. strain SG-4G and its potential for use in enzymatic bioremediation. *Appl. Environ. Microbiol.* **2010**, *76*, 2940.
(67) Wang, Z.; Xu, J.; Li, Y.; Wang, K.; Wang, Y.; Hong, Q.; Li, W. J.; Li, S. P. *Rhodococcus jialingiae* sp. nov., an actinobacterium isolated from

DOI: 10.1021/acs.est.9b01037
Environ. Sci. Technol. 2019, 53, 8695−8705

sludge of a carbendazim wastewater treatment facility. *Int. J. Syst. Evol. Microbiol.* **2010**, *60*, 378−81.
(68) Fang, H.; Wang, Y.; Gao, C.; Yan, H.; Dong, B.; Yu, Y. Isolation and characterization of *Pseudomonas* sp. CBW capable of degrading carbendazim. *Biodegradation* **2010**, *21*, 939−946.
(69) Xiao, W.; Wang, H.; Li, T.; Zhu, Z.; Zhang, J.; He, Z.; Yang, X. Bioremediation of Cd and carbendazim co-contaminated soil by Cd-hyperaccumulator Sedum alfredii associated with carbendazim-degrading bacterial strains. *Environ. Sci. Pollut. Res.* **2013**, *20*, 380−389.
(70) Zhang, Y.; Wang, H.; Wang, X.; Hu, B.; Zhang, C.; Jin, W.; Zhu, S.; Hu, G.; Hong, Q. Identification of the key amino acid sites of the carbendazim hydrolase (MheI) from a novel carbendazim-degrading strain *Mycobacterium* sp. SD-4. *J. Hazard. Mater.* **2017**, *331*, 55−62.
(71) van der Ven, K.; Keil, D.; Moens, L. N.; Van Leemput, K.; van Remortel, P.; De Coen, W. M. Neuropharmaceuticals in the environment: mianserin-induced neuroendocrine disruption in zebrafish (Danio rerio) using cDNA microarrays. *Environ. Toxicol. Chem.* **2006**, *25*, 2645−2652.
(72) Isidori, M.; Parrella, A.; Pistillo, P.; Temussi, F. Effects of ranitidine and its photoderivatives in the aquatic environment. *Environ. Int.* **2009**, *35*, 821−825.
(73) Latch, D. E.; Stender, B. L.; Packer, J. L.; Arnold, W. A.; McNeill, K. Photochemical fate of pharmaceuticals in the environment: cimetidine and ranitidine. *Environ. Sci. Technol.* **2003**, *37*, 3342−3350.
(74) Giebultowicz, J.; Nalecz-Jawecki, G. Occurrence of antidepressant residues in the sewage-impacted Vistula and Utrata rivers and in tap water in Warsaw (Poland). *Ecotoxicol. Environ. Saf.* **2014**, *104*, 103−109.
(75) Babiker, A. G. T.; Duncan, H. J. Influence of soil depth on asulam adsorption and degradation. *Soil Biol. Biochem.* **1977**, *9*, 197−201.
(76) Balba, M. T.; Khan, M. R.; Evans, W. C. The microbial degradation of a sulphanilamide-based herbicide (Asulam). *Biochem. Soc. Trans.* **1979**, *7*, 405−407.
(77) Duben, J.; Rosslenbroich, H. J.; Jenner, G. A new specific fungicide for the control of Botrytis cinerea and related pathogens on Rubus, Ribes and other crops. *Acta Hortic.* **2002**, 325−329.
(78) Leroux, P.; Lanen, C.; Fritz, R. Similarities in the antifungal activities of fenpiclonil, iprodione and tolclofos-methyl against *Botrytis cinerea* and *Fusarium nivale*. *Pestic. Sci.* **1992**, *36*, 255−261.
(79) Rosslenbroich, H. J.; Stuebler, D. Botrytis cinerea-history of chemical control and novel fungicides for its management. *Crop Prot.* **2000**, *19*, 557−561.
(80) Horak, R. E.; Qin, W.; Schauer, A. J.; Armbrust, E. V.; Ingalls, A. E.; Moffett, J. W.; Stahl, D. A.; Devol, A. H. Ammonia oxidation kinetics and temperature sensitivity of a natural marine community dominated by Archaea. *ISME J.* **2013**, *7*, 2023−2033.
(81) Koutsoumanis, K.; Allende, A.; Alvarez-Ordonez, A.; Bolton, D.; Bover-Cid, S.; Chemaly, M.; Davies, R.; Hilbert, F.; Lindqvist, R.; Nauta, M.; Peixe, L.; Ru, G.; Simmons, M.; Skandamis, P.; Suffredini, E.; Cocconcelli, P. S.; Fernandez Escamez, P. S.; Maradona, M. P.; Querol, A.; Suarez, J. E.; Sundh, I.; Vlak, J.; Barizzone, F.; Correia, S.; Herman, L. Update of the list of QPS-recommended biological agents intentionally added to food or feed as notified to EFSA 9: suitability of taxonomic units notified to EFSA until September 2018. *EFSA J.* **2019**, *17*, 5753 DOI: 10.2903/j.efsa.2019.5753.

DOI: 10.1021/acs.est.9b01037
Environ. Sci. Technol. 2019, 53, 8695−8705